Cell Tissue Res (1999) 298:539–548
Digital Object Identifier (DOI) 10.1007/s004419900116

REGULAR ARTICLE

Raimund Strehl · Verena Trautner · Sabine Kloth
Will W. Minuth

Existence of a dense reticular meshwork surrounding the nephron inducer in neonatal rabbit kidney

Received: 17 May 1999 / Accepted: 14 August 1999 / Published online: 7 October 1999

Abstract While more and more humoral factors involved in nephrogenesis are being discovered, there is no detailed knowledge of the morphological structures at the interface of the nephron inducer and the surrounding mesenchyme. For that reason we examined this area in the cortex of neonatal rabbit kidneys by scanning electron-microscopical and transmission electron-microscopical techniques. Our interest was focused on the basal aspect of the collecting duct ampulla and the surrounding competent mesenchyme, where morphogenic signals are to be exchanged during nephron induction. Close contact between these two tissues involved in nephrogenesis is assumed to allow direct cellular contact or diffusion of soluble factors across a short distance. Our data, however, show the presence of a dense fibrillar meshwork around the collecting duct ampulla, spatially separating the inducer and the competent mesenchyme during nephron induction.

Key words Kidney · Collecting duct · Ampulla · Development · Basement membrane · Scanning electron microscopy · Transmission electron microscopy · Rabbit (New Zealand)

Introduction

Three tissues are found in close proximity during nephron induction. The ureter bud-derived collecting duct ampulla (Saxén 1987), the competent mesenchyme (Sorokin and Ekblom 1992), and the developing capillaries sprouting in between (Kloth et al. 1997). Highest in the developmental hierarchy, the collecting duct ampulla controls the histoarchitectural layout of the whole kidney. The process of nephron induction involves an interaction of the ampullar tip and the surrounding mesenchyme. As a visible result, mesenchymal cells condensate and form the comma-shaped and resulting S-shaped bodies that develop into the glomeruli and tubules of the functional nephron (Sorokin and Ekblom 1992). Various factors involved in the induction process are known today. These include structural elements such as fibronectin, laminin, nidogen, and tenascin (Sorokin and Ekblom 1992; Ekblom 1996), and transcription factors such as BF2 (Hatini et al. 1996), Hoxa 11/d11 (Davis et al. 1995), N-*myc* (Stanton et al. 1992), Pax-2 (Rothenpieler and Dressler 1993; Torres et al. 1995), and WT-1 (Kreidberg et al. 1993). Furthermore growth factors and their receptors such as the epidermal growth factors (EGF) receptor (Threadgill et al. 1995), BMP-7 (Dudley et al. 1995), basic fibroblast growth factor (bFGF; Barasch et al. 1997), GDNF (Sanchez et al. >1996; Towers et al. 1998), amylin (Wookey et al. 1998), WNT-4 (Stark et al. 1994), and c-*ret* (Pepicelli et al. 1997; Vainio and Mueller 1997) as well as adhesion molecules such as $\alpha 8\beta 1$-integrin, e-cadherin (Vainio and Mueller 1997), and s-laminin (Noakes et al. 1995). However, the initiation and the complete mechanism of the induction process are yet to be fully understood (Horster et al. 1997).

In places where induction occurred, significant morphological changes take place. The induced mesenchyme condensates to form comma-shaped and then S-shaped bodies. These developing nephrons are located side by side with the collecting duct ampulla but remain spatially separated from the collecting duct. Subsequently the ampullar neck elongates and pushes the tip further toward the capsula fibrosa (Saxén 1987; Aigner et al. 1995). Due to this elongation of the collecting duct, the relative position of the S-shaped bodies shifts from the side of the ampulla toward the ampullar shaft. In that position, further development and eventually the connection of the nephron to the collecting duct system take place.

At the same time, striking morphological and functional changes occur in the collecting duct epithelium in

This investigation was supported by the Deutsche Forschungsgemeinschaft (Mi 331/4–2)

R. Strehl · V. Trautner · S. Kloth · W.W. Minuth (✉)
Department of Anatomy, University of Regensburg,
Universitätsstrasse 31, D-93053 Regensburg, Germany
e-mail: will.minuth@vkl.uni-regensburg.de

this region. Functional P and IC cells develop from embryonic collecting duct epithelium in a transdifferentiation process without intermediate stages (Aigner et al. 1995).

The basal aspect of the ampullar epithelium is especially important as, during nephron induction, morphogenic factors must be exchanged with the surrounding mesenchyme in this region. Histochemical studies show specific antigenic and structural properties in this basal region. The whole basal aspect of the collecting duct epithelium binds peanut lectin (PNA; Kloth et al. 1993), while PNA labeling is only observed at the luminal cell pole of β-type IC cells in mature collecting duct epithelium (LeHir et al. 1982). Recent data show that P_{CD}Amp1 is exclusively expressed at the basal aspect of the collecting duct epithelium (Strehl et al. 1997). Extracellular matrix components such as laminin, collagen type IV, or fibronectin are found in embryonic kidney tissue (Sorokin and Ekblom 1992; Ekblom et al. 1981, 1991), but are not exclusively located around the collecting duct ampulla.

A close and intensive contact between the collecting duct ampulla and the nephrogenic mesenchyme has been postulated during nephron induction (Saxén 1987; Sorokin and Ekblom 1992). Findings of Lehtonen back this assumption, because the ampullar region is not surrounded by a continuously developed basement membrane (Lehtonen 1975). Such a "perforated" basement membrane can suggest cellular communication during induction. On the other hand, Lehtonen shows the presence of ruthenium red-positive fuzzy material around the collecting duct ampulla which causes spatial compartmentation. Little morphological data on the interface of the nephron inducer and the surrounding mesenchyme are available. For that reason we examined the cortex of neonatal rabbit kidneys by scanning electron microscopy and transmission electron microscopy in order to illuminate the spatial organization of the nephron inducer and the neighboring competent mesenchyme. Our findings show an unexpectedly wide intercellular gap between the basal region of the collecting duct ampulla and the surrounding mesenchyme filled with a dense reticular meshwork.

Materials and methods

Tissue preparation

One- to three-day-old New Zealand rabbits were anesthetized with ether and killed by cervical dislocation. Both kidneys were removed immediately. The kidneys were then cut precisely along the corticomedullary axis.

Indirect immunolabeling for confocal laser scanning microscopy

Cryosections (8 µm) of neonatal rabbit kidneys were fixed in ice-cold ethanol and washed. The sections were then incubated in blocking-solution (phosphate-buffered saline, PBS, plus 1% bovine serum albumin, BSA, plus 10% horse serum, HS) for 30 min to saturate nonspecific binding sites. Primary antibodies were applied for 90 min. Fluorescein-isothiocyanate-conjugated (diluted 1:200) species-specific antisera (diluted 1:600; Dianova, Hamburg, Germany) served as detecting antibodies and were applied for 45 min. Following the final washing step, the sections were mounted in FITCguard (Testoc, Chicago, USA) embedding medium and analyzed in the confocal laser scanning microscope at 0.5-µm optical sections. (Axiovert 10 with MR 500 Laserscan; Zeiss, Oberkochen, Germany). For documentation, TriXPan film (Kodak, Hemel-Hempstead, UK) was used.

Immunogold incubation for light microscopy

Cryosections (8 µm) of neonatal rabbit kidney were prepared with a cryomicrotome (Microm, Heidelberg, Germany), fixed in 0.02% glutaraldehyde for 5 min, and washed in PBS. The sections were then incubated in blocking solution (PBS plus 1% BSA plus 10% HS) for 30 min to saturate nonspecific binding sites. Primary antibody was applied for 90 min and the sections were washed again in PBS. A 5- to 6-nm gold-conjugated species-specific secondary antibody (Aurion, Wageningen, Netherlands) served as the detecting antibody and was applied for 45 min at a dilution of 1:10. Following a final washing step in distilled water, the bound gold conjugate was accented by silver enhancement according to the manufacturers instructions (Aurion, Wageningen, Netherlands). The sections were then dehydrated in a graded series of ethanols, embedded in DePex (Serva, Heidelberg, Germany), and analyzed using an Axiovert microscope (Zeiss, Oberkochen, Germany). For documentation, TriXPan film (Kodak, Hemel-Hempstead, UK) was used.

Immunogold preembedding for electron microscopy

Cryosections (20 µm) of neonatal rabbit kidneys were prepared and treated as described above except for the silver enhancement step. The sections were then dehydrated in a graded series of ethanols.

For transmission electron microscopy, the sections were embedded in Epon, which was polymerized at 60°C for 48 h. Ultrathin sections were cut with a glass knife on an OmU3 ultramicrotome (Reichert, Vienna, Austria) and then transferred to 200 lines/inch-mesh nickel grids (SCI, Munich, Germany). Following a contrasting step with 4% uranyl acetate and lead citrate, the sections were examined in an EM 902 transmission electron microscope (Zeiss, Oberkochen, Germany). For documentation, Agfa Scientia EM film (Agfa, Leverkusen, Germany) was used.

For backscatter analysis in the scanning electron microscope (Autrata et al. 1986), the sections were critical-point dried in CO_2 and carbon-coated (Balzers, Liechtenstein, Germany). The specimens were examined in a DSM 940 A scanning electron microscope (Zeiss, Oberkochen, Germany) using a backscattered electron (BSE)-detector (Zeiss, Oberkochen, Germany). For documentation, Agfa Pan 100 film (Agfa, Leverkusen, Germany) was used.

Transmission electron microscopy

For transmission electron microscopy, small pieces of freshly prepared tissue were immediately fixed in 2% paraformaldehyde and 2.5% glutaraldehyde in 0.1 M cacodylate buffer (12 h, 4°C), postfixed in 1% osmium tetroxide in 0.1 M cacodylate buffer, and block-contrasted in 1% uranyl acetate in maleate buffer. The pieces of tissue were then dehydrated in a graded series of ethanols and embedded in Epon, which was polymerized at 60°C for 48 h. Ultrathin sections were cut with a glass knife on an OmU3 ultramicrotome (Reichert, Vienna, Austria) and then transferred to 200 lines/inch-mesh nickel grids (SCI, Munich, Germany). Following a contrasting step with 4% uranyl acetate and lead citrate, the sections were examined in an EM 902 transmission electron microscope (Zeiss, Oberkochen, Germany). For

documentation, Agfa Scientia EM film (Agfa, Leverkusen, Germany) was used.

Scanning electron microscopy

For scanning electron microscopy, precisely oriented pieces of tissue were prepared, fixed in 2% glutaraldehyde in PBS under isotonic conditions (24 h, 4°C), dehydrated in a graded series of ethanols, transferred to acetone, and critical-point dried in CO_2. Finally they were sputter-coated with gold (Polaron, Watford, UK). The specimens were examined in a DSM 940 A scanning electron microscope (Zeiss, Oberkochen, Germany). For documentation, Agfa Pan 100 film (Agfa, Leverkusen, Germany) was used.

Results

The neonatal rabbit kidney is an ideal model for the study of renal developmental processes (Minuth et al. 1988). In a single corticomedullary section, fully embryonic, maturing, and mature structures can be observed. Directly underneath the capsula fibrosa, the earliest stages of nephrogenesis are found. The collecting duct ampullae that are developmentally most important are embedded in nephrogenic mesenchyme and sprouting endothelial cells (Kloth et al. 1997). In close proximity, comma- and S-shaped bodies can be found as the first visible structures of nephron development. Toward the inner cortex, more mature generations of nephrons are visible.

Immunohistochemistry

An important prerequisite for the following studies are precisely oriented sections of neonatal rabbit kidney. The kidney must be cut exactly between both poles from hilus to cortex. Only in such corticomedullary sections can the full length of the maturing collecting ducts be examined from the ampullar tip right underneath the capsule toward the inner medulla, allowing the study of various stages of differentiation. Our interest is focused on the collecting duct ampullae, which are found segmentally arranged underneath the capsula fibrosa in these sections.

The monoclonal antibody (MAb) P_{CD}Amp1 exclusively labels the embryonic ampulla of the collecting duct in neonatal rabbit kidney. The reaction is found in the extracellular matrix of the epithelium and is very intensive along the ampullar tip (Fig. 1a,b). The immunolabel decreases in the ampullar shaft and disappears along the maturing collecting duct. Functionally mature regions of the collecting duct are not labeled by the antibody. The P_{CD}Amp1 antigen has an apparent molecular weight of 39 kDa when solubilized from digested kidney tissue (Strehl et al. 1997). Recent experiments performed with a soluble form of P_{CD}Amp1 secreted by cultured embryonic collecting duct cells show an apparent molecular weight of 78 kDa in sodium dodecyl sulfate-polyacrylamide gel electrophoresis (SDS-PAGE) and a pI between 4.3 and 4.4 in isoelectric focusing (data not shown; R. Strehl, S. Kloth, W. W. Minuth, unpublished work). N-terminal sequencing of trypsin-digested soluble P_{CD}Amp1 revealed one sequence (GVXGFPGADGIPGHPGQ) also found in collagen α2 (IV)-chain precursor from rabbit at position 109–125 (A61228). Two further sequences of soluble P_{CD}Amp1 (FLQXVIG; FYTYER) have no homology with that protein. (N-terminal sequencing in cooperation with PD Dr. Deutzmann, Department of Biochemistry, University of Regensburg).

Surrounding the ampullar tip region where morphogenic interactions occur during nephron induction, the MAb P_{CD}Amp1 immunolabel appears as a wide band and in a specific distribution (Fig. 1a). The label does not align with the course of the basal plasma membrane only but appears to correspond to a basement lamina and further extracellular matrix located in the intercellular space surrounding the ampulla. Confocal laser microscopy of 0.5-µm optical sections yielded comparable results and also show a wide label in the extracellular space surrounding the ampulla (Fig. 1b). Comparative immunohistochemical labeling for P_{CD}Amp1, laminin, collagen type IV, and reticulin shows that only P_{CD}Amp1 appears exclusively in the basement membrane of the collecting duct ampulla (Table 1).

Ultrastructural localization

To substantiate these immunohistochemical findings, immunogold labeling on the electron-microscopical scale was performed. MAb P_{CD}Amp1 does not react on eEpon or LR white sections, so we were forced to use a modified protocol for preembedding incubation. Intracellular compounds are not preserved well by this procedure, but important information can be obtained.

Scanning electron micrographs (BSE image) show a wide P_{CD}Amp1-gold label along the basement membrane of the embryonic collecting duct ampulla, which is strongest in the tip region (Fig. 2a). At a higher magnification, the immunolabel appears as a wide band resembling a densely woven meshwork (Fig. 2b).

In transmission electron micrographs of ultrathin sections of the collecting duct ampulla, no MAb P_{CD}Amp1 label is found on cellular structures (Fig. 2c). The reaction is located along the course of the basement lamina and extends into the intercellular space along fibrillar structures. Not all fibers are labeled with MAb P_{CD}Amp1.

Scanning electron microscopy

The localization of P_{CD}Amp1 in the intercellular space made it necessary to analyze the ampullar surface in more detail and at a higher resolution by scanning electron microscopy. In a first series of experiments, corticomedullary preparations of neonatal rabbit kidney were examined. In the upper portion of Fig. 3a, the capsula fibrosa can be seen. The collecting duct ampulla that is

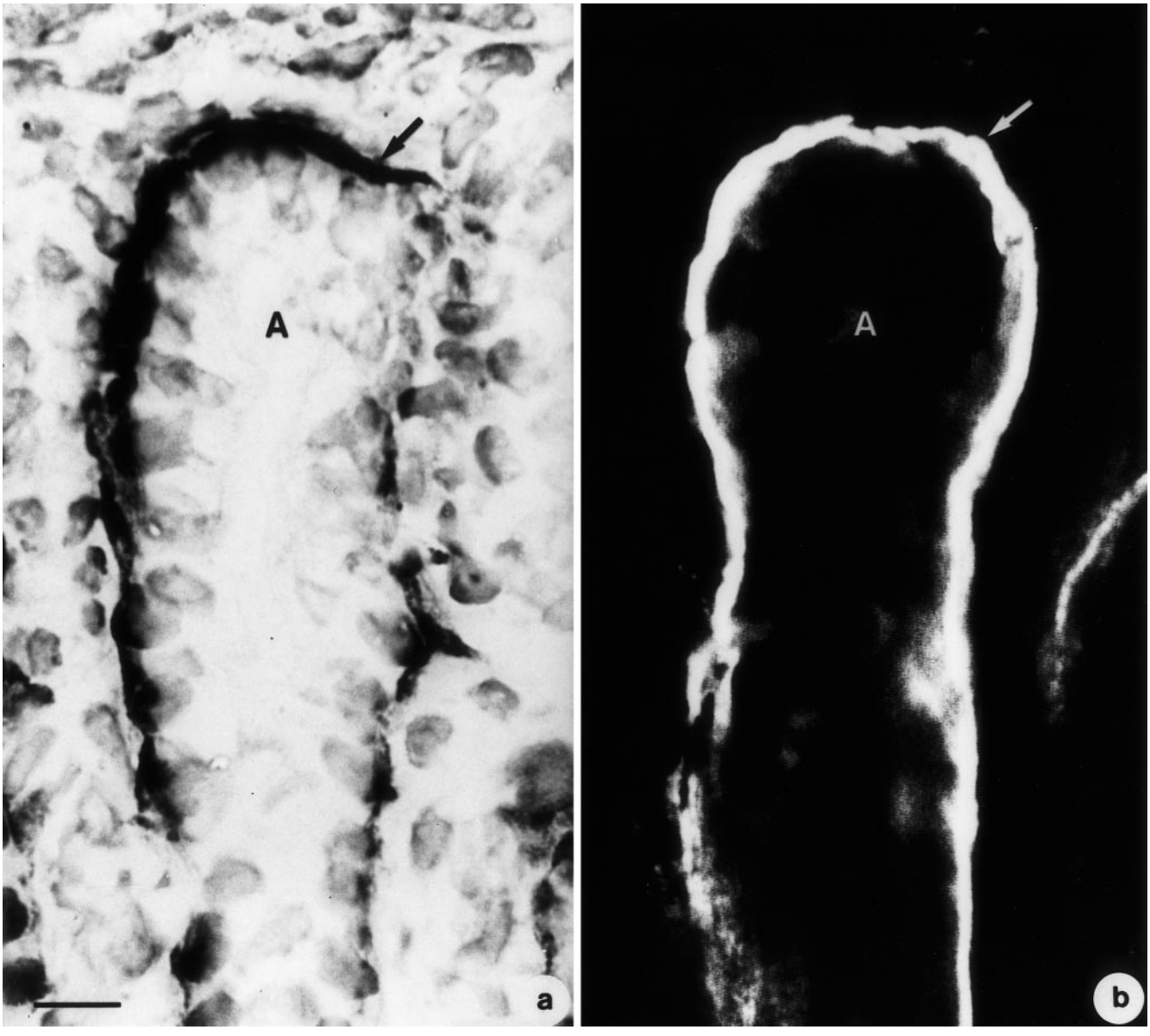

Fig. 1a,b MAb P_{CD}Amp1 immunoreaction in the cortex of neonatal rabbit kidney. **a** Silver-enhanced immunogold incubation. The basement membrane of the embryonic collecting duct ampulla (*A*) is strongly labeled. The immunolabel is wide in the tip region (*arrow*). **b** Confocal laser scanning micrograph of 0.5-µm optical sections. In both preparations the MAb P_{CD}Amp1 label appears as a wide band surrounding the ampullar tip (*arrow*). *Bar* 10 µm

Table 1 Comparative immunohistochemical labeling for extracellular matrix components in the basement membrane (– no reaction, + reaction, ++ strong reaction)

	P_{CD}Amp1	Collagen IV	Reticulin	Laminin
Ampullar tip	++	++	++	+
Ampullar neck	+	++	++	++
Mature collecting duct	–	++	++	++
Developing nephron	–	++	++	++
Mature nephron tubules	–	++	++	++

shown directly underneath the capsula fibrosa is the embryonic part of a maturing collecting duct visible all the way down toward the medulla. The collecting duct ampulla is in an early stage of dichotomous branching. At a higher magnification, the lumen of both ampullar tips can be seen clearly (Fig. 3b). Between the tips of the branching ampulla, a number of mesenchymal cells resting on a dense fibrillar meshwork are observed.

Scanning electron-microscopical analysis of another kidney preparation shows a collecting duct ampulla lo-

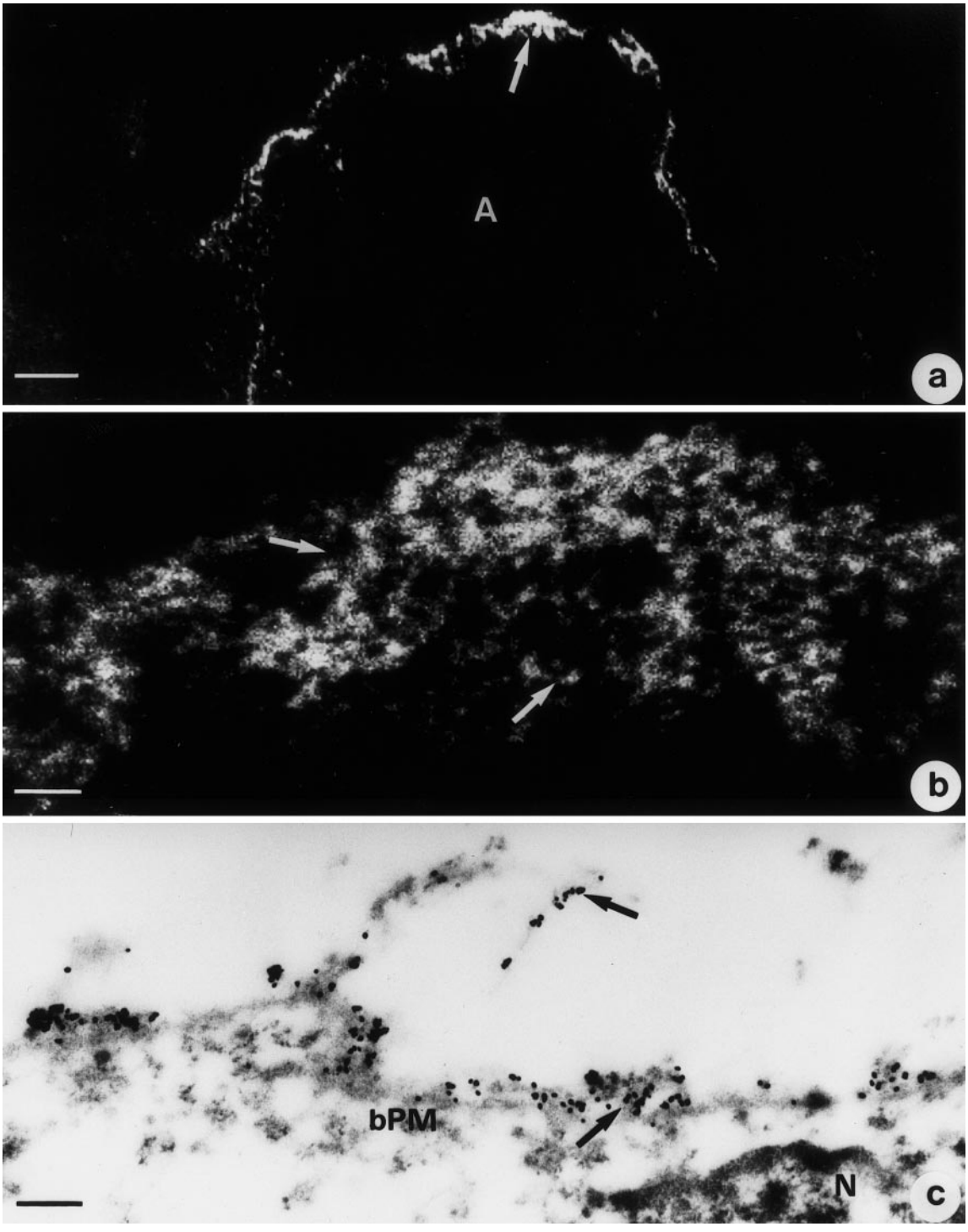

Fig. 2a–c Ultrastructural localization of P_{CD}Amp1. **a** Immunogold preembedding incubation with MAb P_{CD}Amp1. Scanning electron micrograph, backscattered electron image (BSE) of a collecting duct ampulla. The basement membrane of the embryonic collecting duct ampulla (*A*) is clearly labeled. The immunolabel (*arrow*) is strongest in the tip region. *Bar* 5 µm. **b** Higher magnification of the basal aspect of the ampullar tip. The immunolabel (*arrows*) appears as a wide band resembling a densely woven meshwork. *Bar* 500 nm. **c** Immunogold preembedding incubation with MAb P_{CD}Amp1. Transmission electron micrograph. The P_{CD}Amp1 label (*arrows*) is found along the course of the basement lamina. The immunogold label also extends into the intercellular space along fibrillar structures, although not all fibers are labeled with P_{CD}Amp1 (*N* nucleus, *bPM* basal plasma membrane). *Bar* 250 nm

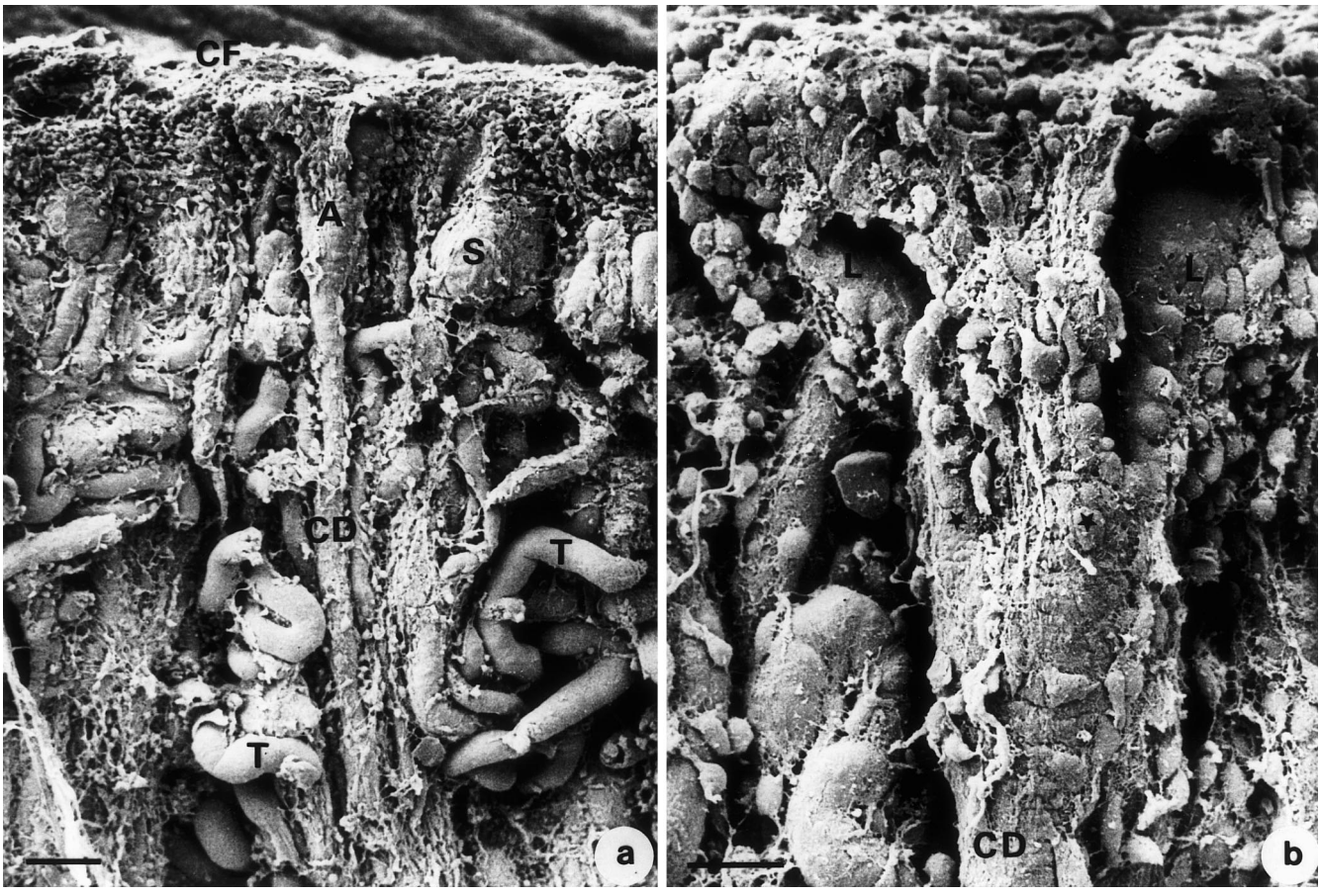

Fig. 3a,b Scanning electron micrographs of the cortex of neonatal rabbit kidney. **a** Overview. The collecting duct ampulla (*A*) which can be seen directly underneath the capsula fibrosa (*CF*) is the embryonic part of a maturing collecting duct (*CD*), which is visible all the way down toward the medulla. Laterally a developing nephron (*S*) and convoluted parts of developing tubules (*T*) can be observed. *Bar* 50 µm. **b** Higher magnification of the collecting duct ampulla in an early stage of dichotomous branching (*stars*). The lumen (L) of both ampullar tips can be seen clearly. *At the bottom*, part of the maturing collecting duct (*CD*) can be seen. *Bar* 20 µm

cated directly underneath the capsula fibrosa (Fig. 4a). The opened lumen in the ampullar tip region is lined by a continuous layer of epithelial cells. In all specimens examined, the epithelial cells were found to rest on a strikingly thick and structured basement membrane separating the collecting duct ampulla from the surrounding endothelial and mesenchymal cells.

At a higher magnification, a thick meshwork of fibers surrounding the collecting duct ampulla becomes clearly visible (Fig. 4b). This resembles a reticular lamina containing thick fibers and a large variety of thinner branching fibers reminding of collagenous and reticular structures. In all preparations the fibrillar meshwork is especially prominent at the tips of the ampulla, while its thickness decreases in the ampullar shaft region. In the maturing and mature collecting duct, the fibrillar material, while still visible, is much thinner than in the ampulla.

To verify whether the fibrillar meshwork is restricted to the collecting duct, other developing renal tubules were examined in detail in the scanning electron microscope. The scanning electron micrograph of the surface of a convoluted tubule segment shows a surprisingly smooth surface (Fig. 4c). At a higher magnification, no fibrillar structures comparable with the meshwork around the collecting duct ampulla can be seen (Fig. 4d).

Transmission electron microscopy

In the next series of experiments, the structure of the fibrillar meshwork was further examined in the transmission electron microscope (Fig. 5). Longitudinal sections of the ampullar tip (Fig. 5a) and the ampullar side (Fig. 5b) show epithelial cells resting on a thick basement membrane. The basement lamina shows discontinuities(Fig. 5a, arrows). Toward the interstitium, a dense layer of various types of fibers differing in thickness and structure are visible. They appear to be part of a reticular lamina. The fibers are in direct contact with the basement lamina and even penetrate it in some places to be in contact with the basal plasma membrane of the ampullar collecting duct cells. The mean distance between epithelium and mesenchyme in the ampullar tip region is 1.6 µm (n=25), with values ranging from 0.23 µm to 3.18 µm. While the fibrillar meshwork is very prominent

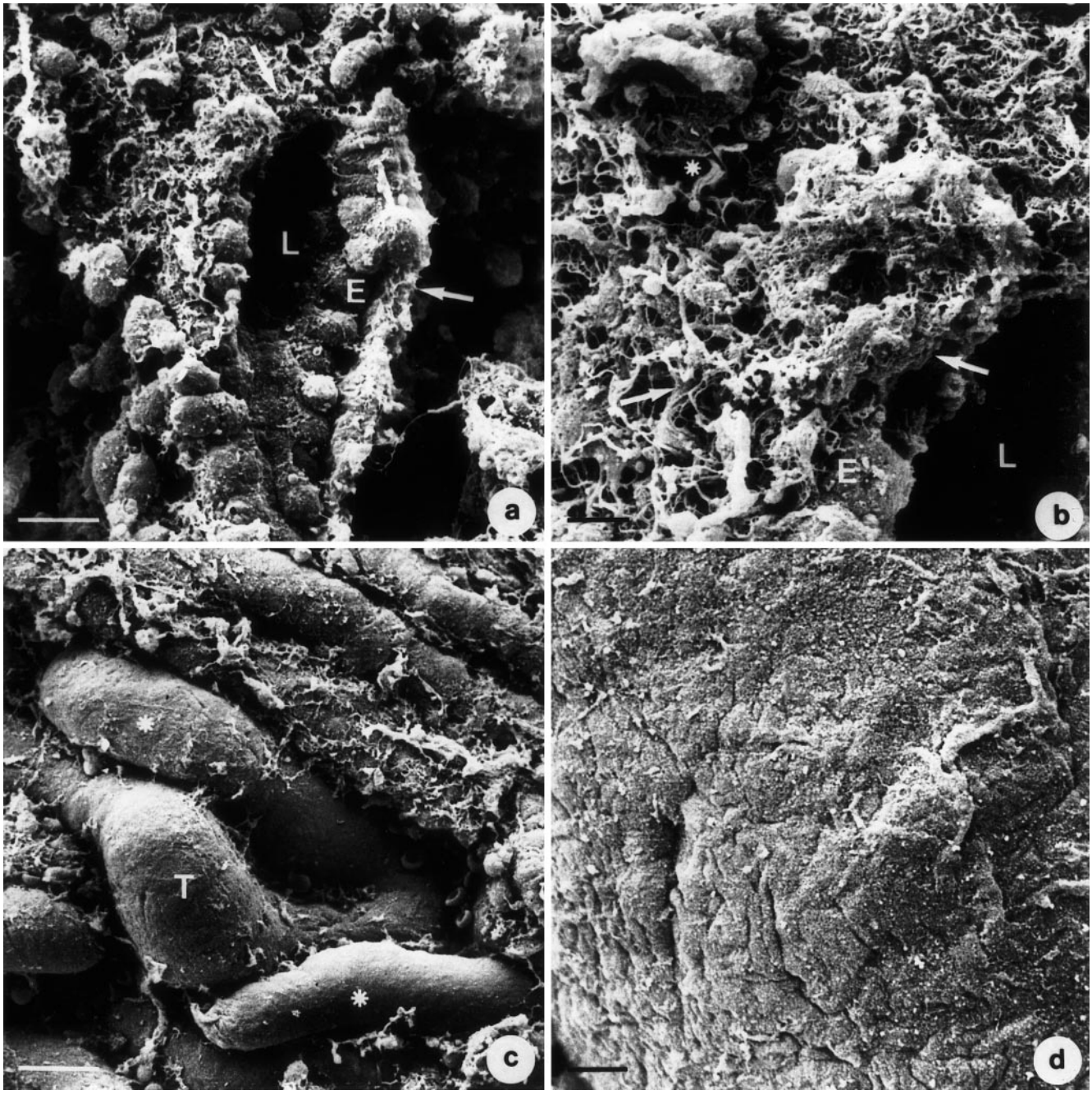

Fig. 4a,**b** Scanning electron micrographs of the fibrillar meshwork around the collecting duct ampulla. **a** The overview shows an opened collecting duct ampulla. The lumen (*L*) and the layer of epithelial cells (*E*) can be seen clearly. The ampulla is surrounded by an unexpectedly thick and structured basement membrane (*arrows*). *Bar* 10 µm. **b** Higher magnification of the wall of the collecting duct ampulla showing the lumen (*L*), a cross section of the layer of epithelial cells (*E*), and the three-dimensional extension of the surrounding reticular lamina (*arrows*). The basement membrane consists of a variety of fibers differing in thickness (*star*). *Bar* 2.5 µm. **c**,**d** Scanning electron micrographs of the smooth surface of the convoluted part of the nephron tubules. **c** The overview shows the surface of developing nephron tubules (*T*). A fibrillar meshwork cannot be seen here (*stars*). *Bar* 10 µm. **d** Higher magnification micrograph of the surface of a developing nephron tubule showing a very smooth, fiber-free structure. *Bar* 2.5 µm

at the ampullar tip (Fig. 5a), a decrease in thickness can be observed at the side of the ampulla (Fig. 5b). In the maturing collecting duct below the ampullar shaft, no discontinuities can be observed in the basement lamina (Fig. 5c). The reticular lamina is much thinner in this region than it is at the ampullar tip (Fig. 5a).

Comparing the basement membrane of the convoluted part of a developing tubule (Fig. 5d) with that of the ampullar tip (Fig. 5a), it is obvious that discontinuities in the basement lamina along with a thick reticular lamina are specific for the embryonic collecting duct and cannot be observed on tubules.

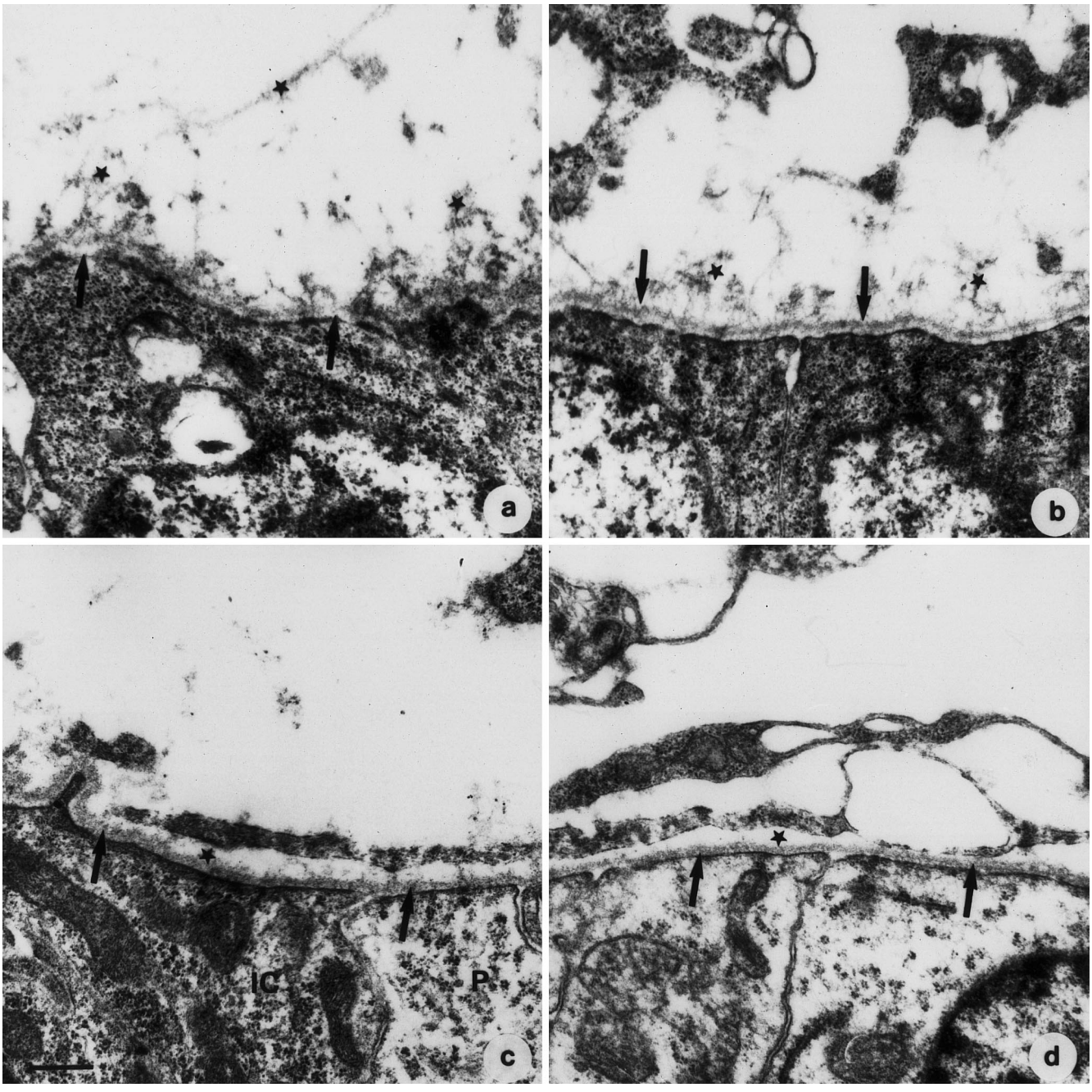

Fig. 5a–d Transmission electron micrographs of the basal aspect of **a** the ampullar tip, **b** the ampullar side, **c** maturing collecting duct, and **d** the convoluted part of a developing nephron. **a** In the ampullar tip region, discontinuities in the basement lamina are visible (*arrows*). The reticular lamina (*stars*) is very thick and densely woven in this region, confirming our findings obtained by scanning electron microscopy. **b** At the lateral aspects of the ampulla, a continuously developed basement lamina can be found (*arrows*). The thickness of the reticular lamina (*stars*) decreases in this region. **c** Maturing collecting duct. A continuous basement lamina (*arrows*) in combination with a drastically reduced reticular lamina (*star*) can be found here (*P* principal cell, *IC* intercalated cell). **d** At the basal aspect of the convoluted part of a developing nephron, a continuous basement lamina (*arrows*) but no reticular lamina (*star*) can be found. *Bar* 450 nm

Discussion

During kidney organogenesis, nephrons are generated by a morphogenic interaction of the ampullar tip with the surrounding mesenchyme (Saxén 1987; Sorokin and Ekblom 1992). Although a number of factors involved in the process of nephrogenesis are known today, the mechanism of the induction remains unclear. In vitro experiments with a heterogeneous inducer such as spinal cord show that induction occurs by direct cell-to-cell contact (Wartiovaara et al. 1972). For the kidney, though, no experimental data are available in this field. Another possibility is the exchange of humoral morphogens by diffusion across the intercellular space (Weller et al. 1991).

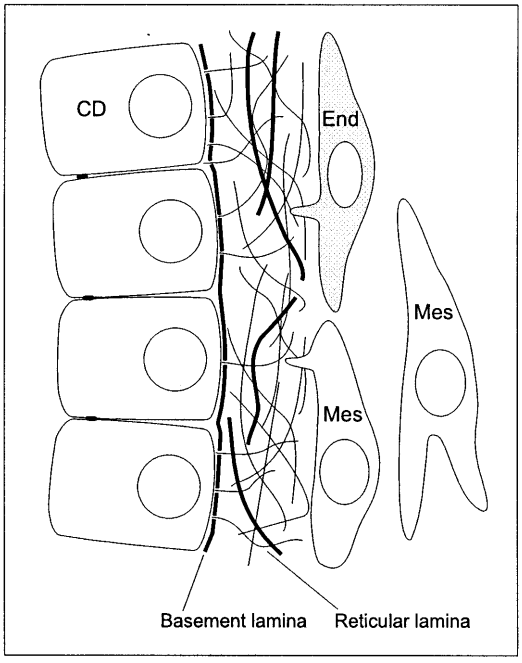

Fig. 6 Schematic showing the interface of the collecting duct ampulla and the competent mesenchyme. The epithelial cells of the embryonic ampullar collecting duct (*CD*) rest on a basement membrane consisting of a basement lamina and a thick and densely woven reticular lamina. They are spatially separated from the endothelial cells (*End*) and the competent mesenchymal cells (*Mes*)

The fact that morphogenic signals have to be exchanged either by diffusion or through cell-cell contacts during nephrogenesis suggests a close spatial interaction of the tissues involved.

The scanning- and electron-microscopical analysis presented here for the neonatal rabbit kidney shows unexpected morphological conditions for induction between the collecting duct ampulla and the mesenchyme. Scanning electron micrographs of the basal aspect of the collecting duct ampulla show that the nephron inducer is surrounded by a dense meshwork of fibrillar material (Figs. 3, 4). The mean distance between the tissues is 1.6 µm. Transmission electron micrographs show fibrillar material filling a wide intercellular gap around the ampulla The fibers are found in direct contact with the plasma membrane of the ampullar epithelial cells (Fig. 5a,b) as well as the competent mesenchymal cells. The meshwork seems to bridge the wide intercellular space and may establish an extracellular connection (Fig. 6). It may be part of the induction process either as an active partner or as a mediator. The role of the extracellular matrix as part of the inductive molecular mechanisms is being discussed (Sorokin and Ekblom 1992; Fouser and Avner 1993) and our findings may add additional evidence to this theory. The composition and possible functions of the meshwork surrounding the collecting duct ampulla need to be examined in greater detail.

Acknowledgments The skillful technical assistance of Mrs. Elfriede Eckert, Vera Koenicke, and Irmgard Hertting is gratefully acknowledged.

References

Aigner J, Kloth S, Minuth WW (1995) Transitional differentiation patterns of principal and intercalated cells during renal collecting duct development. Epithelial Cell Biol 4:121–130

Autrata R, Walther P, Kriz S, Mueller M (1986) A BSE-scintillation detector in the (S)TEM. Scanning 8:3–8

Barasch J, Quiao J, McWilliams G, Chen D, Oliver JA, Herzlinger D (1997) Uretric bud stem cells secrete multiple factors, including bFGF, which rescue renal progenitors from apoptosis. Am J Physiol 273(2):F757–767

Davis AP, Witte DP, Hsieh-Li HM, Potter SS, Capecchi MR (1995) Absence of radius and ulna in mice lacking hoxa-11 and hoxad-11. Nature 375:791–795

Dudley AT, Lyons KM, Robertson EJ (1995) A requirement for BMP-7 during development of the mammalian kidney and eye. Genes Dev 9:2795–2807

Ekblom P (1996) Extracellular and cell adhesion molecules in nephrognesis. Exp Nephrol 4:92–96

Ekblom P, Lehtonen E, Saxén L, Timpl R (1981) Shift in collagen type as an early response to induction of the metanephric mesenchyme. J Cell Biol 89:276–283

Ekblom P, Klein G, Ekblom M, Sorokin L (1991) Laminin isoforms and their receptors in the developing kidney. Am J Kidney Dis 17:603–605

Fouser I, Avner ED (1993) Normal and abnormal nephrogenesis. Am J Kidney Dis 21(1):64–70

Hatini V, Huh SO, Herzlinger D, Soares VC, Lai E (1996) Essential role of stromal mesenchyme in kidney morphogenesis revealed by targeted disruption of Winged Helix transcription factor BF-2. Genes Dev 10:1467–1478

Horster M, Huber S, Tschöp J, Dittrich G, Braun G (1997) Epithelial nephrogenesis. Pflugers Arch 434:647–660

Kloth S, Aigner J, Brandt E, Moll R, Minuth WW (1993) Histochemical markers reveal an unexpected heterogenous composition of the renal embryonic collecting duct epithelium. Kidney Int 44:527–536

Kloth S, Ebenbeck C, Monzer J, de Vries U, Minuth WW (1997) Three dimensional organization of the developing vasculature of the kidney. Cell Tissue Res 287:193–201

Kreidberg JA, Sariola H, Loring JM, Maeda M, Pelletier J, Housman D, Jaenisch R (1993) WT-1 is required for early kidney development. Cell 74:679–691

LeHir M, Kaissling B, Koeppen BM, Wade JB (1982) Binding of peanut lectin to specific epithelial cell types in kidney. Am J Physiol 242:C117–C120

Lehtonen E (1975) Epithelio-mesenchymal interface during mouse kidney tubule induction in vivo. J Embryol Exp Morphol 34:695–705

Minuth WW, Gilbert P, Gross P (1988) Appearance of specific proteins in the apical plasma membrane of cultured renal collecting duct principal cell epithelium after chronic administration of aldosterone and arginine vasopressin. Differentiation 38:194–202

Noakes PG, Miner JH, Gautam M, Cunningham JM, Sanes J, Merlie JP (1995) The renal glomerulus of mice lacking s-laminin/lamininβ2: nephrosis despite glomerular compensation by laminin β1. Nat Genet 10:400–406

Pepicelli CV, Kispert A, Rowitch DH, McMahon AP (1997) GDNF induces branching and increased cell proliferation in the ureter of the mouse. Dev Biol 192(1):193–198

Rothenpieler UW, Dressler GR (1993) Pax-2 is required for mesenchyme-to-epithelium conversion during kidney development. Development 119(3):711–720

Sanchez MP, Silos-Santiago I, Frisen J, He B, Lira SA, Barbacid M (1996) Renal agenesis and the absence of enteric neurons in mice lacking GDNF. Nature 382:70–73

Saxén L (1987) Organogenesis of the kidney. (Developmental and cell biology series) Cambridge University Press, Cambridge

Sorokin L, Ekblom P (1992) Development of tubular and glomerular cells of the kidney. Kidney Int 41:657–664

Stanton BR, Perkins AS, Tessarollo L, Sassoon DA, Parada LF (1992) Loss of N-*myc* function results in embryonic lethality and failure of the epithelial component of the embryo to develop. Genes Dev 6:2235–2247

Stark K, Vainio S, Vassileva G, McMahon AP (1994) Epithelial transformation of metanephric mesenchayme in the developing kidney regulated by Wnt-4. Nature 372:679–683

Strehl R, Kloth S, Aigner J, Steiner P, Minuth WW (1997) P_{CD}amp1, a new antigen at the interface of the embryonic collecting duct epithelium and the nephrogenic mesenchyme. Kidney Int 52:1469–1477

Threadgill DW, Dlugosz AA, Hansen LA, Tennenbaum T, Lichti U, Yee D, LaMantia C, Mourton T, Herrup K, Harris RC (1995) Targeted disruption of mouse EGF receptor: effect of genetic background on mutant phenotype. Science 269:230–234

Torres M, Gomez-Pardo E, Dressler GR, Gruss P (1995) Pax-2 controls multiple steps of urogenital development. Development 121:4057–4065

Towers PR, Woolf AS, Hardman P (1998) GDNF stimulates ureteric bud outgrowth and enhances survival of ureteric bud cells in vitro. Exp Nephrology 6:337–351

Vainio S, Mueller U (1997) Inductive tissue interactions, cell signaling and the control of kidney organogenesis. Cell 90:975–978

Wartiovaara J, Lehtonen E, Nordling S, Saxén L (1972) Do membrane filters prevent cell contacts? Nature 238:407–408

Weller A, Sorokin L, Illgen EM, Ekblom P (1991) Development of mouse embryonic kidney in organ culture and modulation of development by soluble growth factor. Dev Biol 144(2): 248–261

Wookey PJ, Tikellis C, Nobes M, Casley D, Cooper ME, Darby IA (1998) Amylin as a growth factor during fetal and postnatal development of the rat kidney. Kidney Int 53:25–30